Title

A disease-associated mutation in fibrillin-1 differentially regulates integrin-mediated cell adhesion

Permalink

https://escholarship.org/uc/item/4tr4s37p

Journal

Journal of Biological Chemistry, 294(48)

ISSN

0021-9258

Authors

Del Cid, Joselyn S
Reed, Nilgun Isik
Molnar, Kathleen
et al.

Publication Date

2019-11-01

DOI

10.1074/jbc.ra119.011109

Peer reviewed

A disease-associated mutation in fibrillin-1 differentially regulates integrin-mediated cell adhesion

Joselyn S. Del Cid[‡1], Nilgun Isik Reed[‡], Kathleen Molnar[§2], Sean Liu[‡], Bobo Dang[§], Sacha A. Jensen[¶], William DeGrado[§], Penny A. Handford[¶], Dean Sheppard[‡3], and Aparna B. Sundaram[‡3,4]

From the ‡Department of Cell Biology, University of California San Francisco, San Francisco, California 94158, the §Department of Pharmaceutical Chemistry, University of California San Francisco, San Francisco, California 94518, and the ¶Department of Biochemistry, University of Oxford, Oxford OX1 3QU, United Kingdom

Edited by Enrique M. De La Cruz

Fibrillins serve as scaffolds for the assembly of elastic fibers that contribute to the maintenance of tissue homeostasis and regulate growth factor signaling in the extracellular space. Fibrillin-1 is a modular glycoprotein that includes 7 latent transforming growth factor β (TGFβ)-binding protein-like (TB) domains and mediates cell adhesion through integrin binding to the RGD motif in its 4th TB domain. A subset of missense mutations within TB4 cause stiff skin syndrome (SSS), a rare autosomal dominant form of scleroderma. The fibrotic phenotype is thought to be regulated by changes in the ability of fibrillin-1 to mediate integrin binding. We characterized the ability of each RGD-binding integrin to mediate cell adhesion to fibrillin-1 or a disease-causing variant. Our data show that 7 of the 8 RGD-binding integrins can mediate adhesion to fibrillin-1. A single amino acid substitution responsible for SSS (W1570C) markedly inhibited adhesion mediated by integrins $\alpha5\beta1$, $\alpha v\beta5$, and $\alpha v\beta6$, partially inhibited adhesion mediated by $\alpha v\beta1$, and did not inhibit adhesion mediated by $\alpha8\beta1$ or $\alpha IIb\beta3$. Adhesion mediated by integrin $\alpha v\beta3$ depended on the cell surface expression level. In the SSS mutant background, the presence of a cysteine residue in place of highly conserved tryptophan 1570 alters the conformation of the region containing the exposed RGD sequence within the same domain to differentially affect fibrillin's interactions with distinct RGD-binding integrins.

Fibrillins are large and multidomain glycoproteins that are central organizers of elastin-containing microfibrils. They serve as scaffolds for the assembly of multiprotein complexes that contribute to the maintenance of tissue homeostasis and the regulation of growth factor signaling in the extracellular space (1). Three different variants of fibrillin are present in humans: fibrillin-1 (FBN1),[5] fibrillin-2 (FBN2), and fibrillin-3 (FBN3) (2). All three variants are ~350-kDa proteins that are structurally related to the latent TGFβ-binding proteins (LTBPs). Fibrillin-1 is the major component of tensile-strength transmitting 10–12-nm microfibrils of the ECM and many mutations in the *FBN1* gene cause Marfan syndrome (3–5). Fibrillin-2 has been shown to play a more primary role in the formation of microfibrils during embryonic development and mutations in this variant lead to congenital contractural arachnodactyly (6). Much less is known about fibrillin-3; like fibrillin-2, its expression pattern is highest in fetal tissues and it localizes predominately to the brain (7).

The genomic organization of fibrillin-1 was originally described in 1993 by Pereira *et al.* (8). Fibrillin-1 was shown to be structurally composed of 5 distinct domains. Like the LTBPs and many other extracellular and cell-surface proteins, fibrillin-1 contains a large number of cysteine-rich sequences that are homologous to epidermal growth factor (EGF). These EGF-like domains compose ~75% of the protein and of the 47 EGF-like domains, 43 are calcium binding (cbEGF) (9). Fibrillin-1 also contains 7 TGFβ-binding protein-like domains (TB) that are similar to domains found in the LTBP family (10). The remaining domains exist at lower frequency: a fibrillin unique N-terminal (FUN) domain, a proline-rich domain, and 2 hybrid domains that share similarities with both the EGF-like and TB domains (11).

The majority of FBN1 mutations have been linked to the development of Marfan syndrome, a connective tissue disorder that results in cardiovascular, skeletal, and ocular defects (3, 4). However, a subset of missense mutations within a single domain, TB4, result in stiff skin syndrome (SSS), a vastly phenotypically dissimilar disease characterized by short stature, joint stiffness, and thickening of the skin (12, 13). TB4 is the only domain in fibrillin-1 that contains an exposed arginine, glycine, aspartic acid tri-peptide (RGD), a common recognition motif for binding a subset of members of the integrin family (14). This observation has led to the suggestion that SSS might

Figure 1. The fibrillin-1 sequence is composed predominantly by 47 EGF-like domains, 43 that are Ca²⁺ binding. The repeating structural domains of fibrillin-1 are defined at the *top* of the figure. The fragment cbEGF19–cbEGF25, containing the 4th TB repeat, was purified in a human mammalian system using the adjoining His tag. The amino acid sequence for part of domain TB4 denotes the location of the RGD domain and the subsequent tryptophan that is mutated in the SSS background.

be due to altered interactions between fibrillin-1 and one or more integrins (12). Further support for this hypothesis was provided by the observation that mice with a knock-in of the most common SSS disease-inducing mutation, and mice with a presumed loss-of-integrin–binding mutation (knock-in of a glutamic acid for aspartic acid in the RGD domain) each developed increases in skin stiffness and thickness reminiscent of human SSS (15).

Prior reports have suggested that three integrins, $\alpha v\beta 3$, $\alpha 5\beta 1$, and $\alpha v\beta 6$, can bind to the RGD domain of fibrillin-1. The binding capacities of integrins $\alpha v\beta 3$ and $\alpha 5\beta 1$ were determined through cell-based assays measuring adhesion to fibrillin-1 or through changes in cell spreading and cytoskeletal rearrangement (13, 16, 17). A more quantitative approach using surface plasmon resonance analysis in 2007 by Jovanovic *et al.* (18, 19) concluded that $\alpha v\beta 6$ can also bind fibrillin and has a k_d value of 0.45 μM for fragments containing the TB4 domain. However, there are 8 well-characterized RGD-binding integrins; $\alpha v\beta 1$, $\alpha v\beta 3$, $\alpha v\beta 5$, $\alpha v\beta 6$, $\alpha v\beta 8$, $\alpha 5\beta 1$, $\alpha 8\beta 1$, and $\alpha IIb\beta 3$ (20). The relative effectiveness of each of these integrins to bind fibrillin-1, and the effects of disease-causing mutations on interactions with the full range of fibrillin-1–binding integrins has not been systematically evaluated.

In this paper, we developed cell-based assays to systematically study the ability of each of the RGD-binding integrins to mediate cell adhesion to fibrillin-1. We further sought to determine how the W1570C SSS substitution in the TB4 domain might differentially affect binding to each fibrillin–binding integrin. We found that 7 of the 8 RGD-binding integrins can mediate adhesion to fibrillin-1, but that adhesion mediated by 4 of these ($\alpha v\beta 1$, $\alpha v\beta 5$, $\alpha v\beta 6$, and $\alpha 5\beta 1$) and potentially $\alpha v\beta 3$ (dependent on local protein-ligand stoichiometry) is affected by the SSS mutation. Our findings thus identify a subset of RGD-binding integrins through which inhibition of binding to mutant fibrillin could contribute to the development of SSS.

Results

Purification of fibrillin-1 fragments from mammalian cells

To determine which members of the RGD-binding integrin subfamily recognize the RGD sequence in fibrillin-1, human recombinant fragments containing domains cbEGF19–cbEGF25, which includes TB4 containing the RGD motif, was purified from HEK293FS cells (Fig. 1*A*). Fragments were puri-

fied for the WT protein, the SSS disease-causing mutant and the RGE, loss-of-integrin–binding control mutant.

Characterization of cell-based systems

We utilized cell-adhesion assays to systematically evaluate the ability of the 8 known integrins that bind to RGD-containing ligands to bind to fibrillin-1. For 6 of these, $\alpha 5\beta 1$, $\alpha 8\beta 1$, $\alpha v\beta 3$, $\alpha v\beta 5$, $\alpha v\beta 6$, and $\alpha v\beta 8$, we used SW480 cells, a colon cancer cell line that endogenously expresses $\alpha v\beta 5$ and $\alpha 5\beta 1$ but does not express any of the remaining RGD-binding integrins (Fig. 2, *A* and *C*). We transfected SW480 cells to express individual integrin subunits, $\beta 8$, $\beta 3$, $\beta 6$, or $\alpha 8$, as previously described (21–24), to induce high cell-surface expression levels of $\alpha 8\beta 1$, $\alpha v\beta 3$, $\alpha v\beta 6$, and $\alpha v\beta 8$, respectively (Fig. 2*B*). SW480 cells cannot be induced to express functional $\alpha v\beta 1$ or $\alpha IIb\beta 3$. Integrin $\alpha v\beta 1$ was therefore evaluated using human dermal fibroblasts (HDF), which endogenously express functional $\alpha v\beta 1$ (Fig. 2*E*). They also express integrins, $\alpha v\beta 3$, $\alpha v\beta 5$, and $\alpha 5\beta 1$ (Fig. 2*D*). Integrin $\alpha IIb\beta 3$ has been shown to be expressed on the cell surface of platelets and was evaluated using human platelets freshly isolated from whole blood (25).

7 of 8 RGD integrins mediate cell adhesion to WT fibrillin-1

To assess the potency of each integrin to individually mediate adhesion to WT fibrillin-1 fragments, we isolated the effects of each integrin by blocking every other RGD-binding integrin expressed by the utilized cell type and quantified adhesion to dishes coated with a wide range of fragment concentrations (4.5–450 nM). Thus, for WT SW480 cells, adhesion mediated by $\alpha 5\beta 1$ was determined in the presence of blocking antibody to $\alpha v\beta 5$ (ALULA) and adhesion mediated by $\alpha v\beta 5$ was determined in the presence of blocking antibody to $\alpha 5\beta 1$ (P1D6). For SW480 cells transfected to express additional integrins, adhesion mediated by the heterologously expressed integrin was assessed in the presence of blocking antibodies to both $\alpha 5\beta 1$ and $\alpha v\beta 5$ (Table 1). In each panel we compare data for adhesion of the cell line used in the absence of any blocking antibody to adhesion in the presence of blocking antibodies against all other expressed RGD-binding integrins (Fig. 3). We found that $\alpha v\beta 5$ and $\alpha v\beta 3$ were both highly effective receptors for WT fibrillin-1 (Fig. 3, *A* and *B*). $\alpha 5\beta 1$ and $\alpha 8\beta 1$ also mediated adhesion, but to a lesser degree (Fig. 3, *C* and *D*). The comparatively weak binding mediated by $\alpha 5\beta 1$ could be explained by the relatively
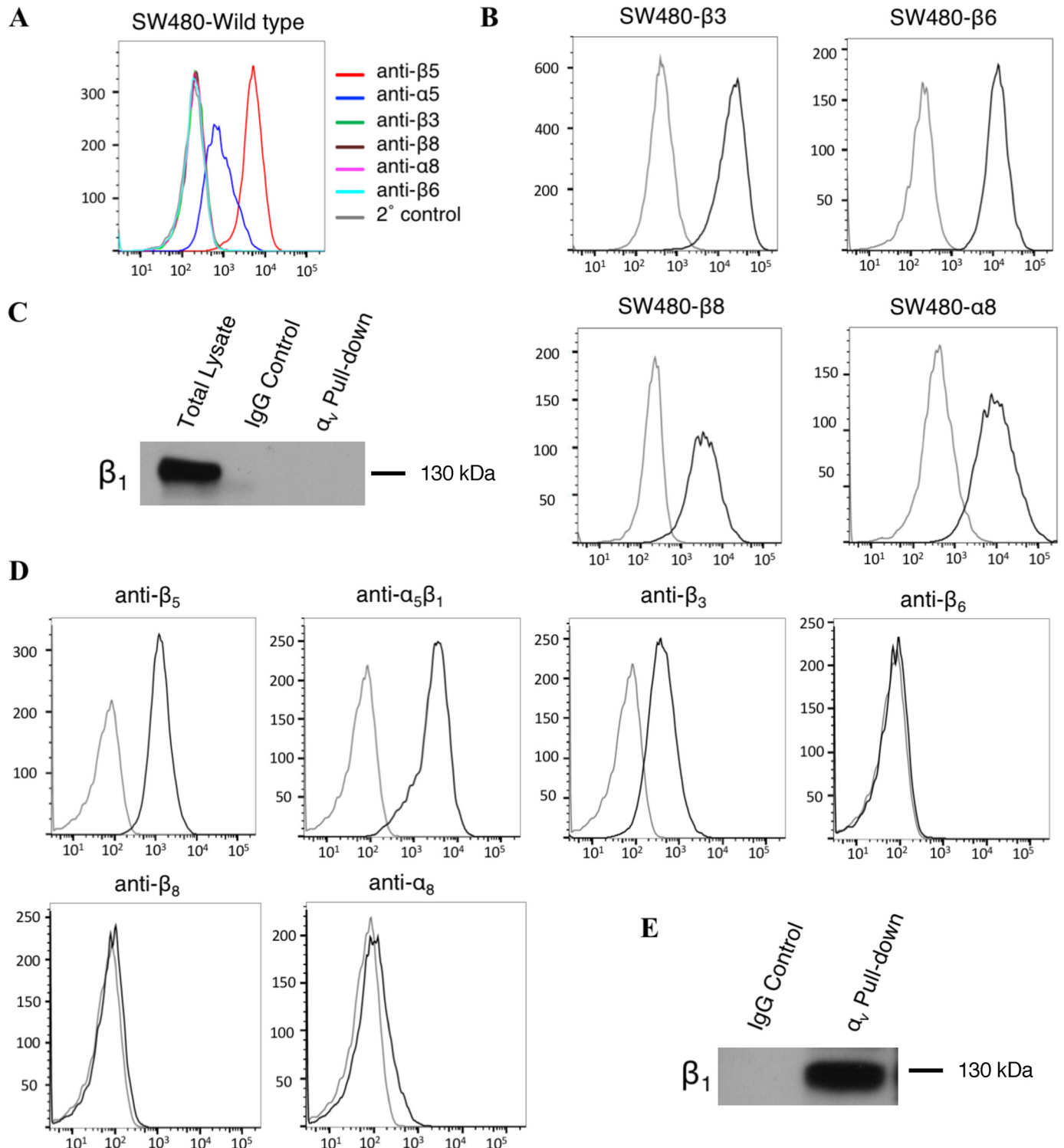
Figure 2. *A,* SW480 cells show high surface expression of both endogenous and *B,* transfected integrin subunits. Cells were labeled in suspension with primary antibodies against specific cell-surface integrins followed by incubation with a secondary antibody conjugated to PE. Cells were analyzed by flow cytometry and gated for live cells. Representative histograms of PE expression *versus* cell count are shown, *x* axis: PE expression (mean fluorescence intensity), *y* axis: cell count. *C,* cell surface expression of $\alpha v \beta 1$ was measured by immunoprecipitation-Western blotting. SW480 cells were lysed in RIPA buffer and incubated with a primary antibody against αv. Sepharose G beads were used to pulldown primary antibody, the resulting solution was run on 8% SDS-PAGE and Western blotted for $\beta 1$ expression. *D,* HDF show varying levels of cell-surface expression of the RGD-binding integrin family. *E,* cell-surface expression of $\alpha v \beta 1$ in HDF was measured by immunoprecipitation-Western blotting as described above.

low expression of $\alpha 5 \beta 1$ in WT SW480 cells. $\alpha v \beta 6$ only weakly mediated adhesion, and $\alpha v \beta 8$ did not mediate adhesion at all (Fig. 3, *E* and *F*).

Evaluations of integrins $\alpha v \beta 1$ and $\alpha IIb \beta 3$ were completed using cell-adhesion assays with HDF and human platelets, respectively. The individual contribution of $\alpha v \beta 1$ was com-

Table 1

Antibody blockade for integrin isolation in cell-adhesion assays

Cells were exposed to combination antibody treatments for isolation of specific integrin-mediated adhesion. All antibodies were added at 10 μg/ml to cells suspended in FBS-free medium and incubated on ice for 10 min before plating on fibrillin-1–coated plates. C8 is a small molecule inhibitor of αvβ1 and was added at 10 μM.

Integrin	Cell line	Antibodies for integrin isolation	Antibodies for complete blockade
α5β1	SW480	ALULA	ALULA + P1D6
αvβ5	SW480	P1D6	ALULA + P1D6
αvβ3	SW480-β3	ALULA + P1D6	ALULA + P1D6 + AXUM2
αvβ6	SW480-β6	ALULA + P1D6	ALULA + P1D6 + 3G9
α8β1	SW480-α8	ALULA + P1D6	ALULA + P1D6 + YZ83
αvβ8	SW480-β8	ALULA + P1D6	ALULA + P1D6 + ADWA-11
αvβ1	HDF	ALULA + P1D6 + AXUM2	L230 + P5D2
α5β1	HDF	L230	L230 + P5D2
αvβ5	HDF	P1D6 + AXUM2 + C8	ALULA + P1D6 + AXUM2 + C8
αvβ3	HDF	ALULA + P1D6 + C8	ALULA + P1D6 + AXUM2 + C8
αIIbβ3	Human platelets	L230 + P5D2	L230 + P5D2 + 10E5
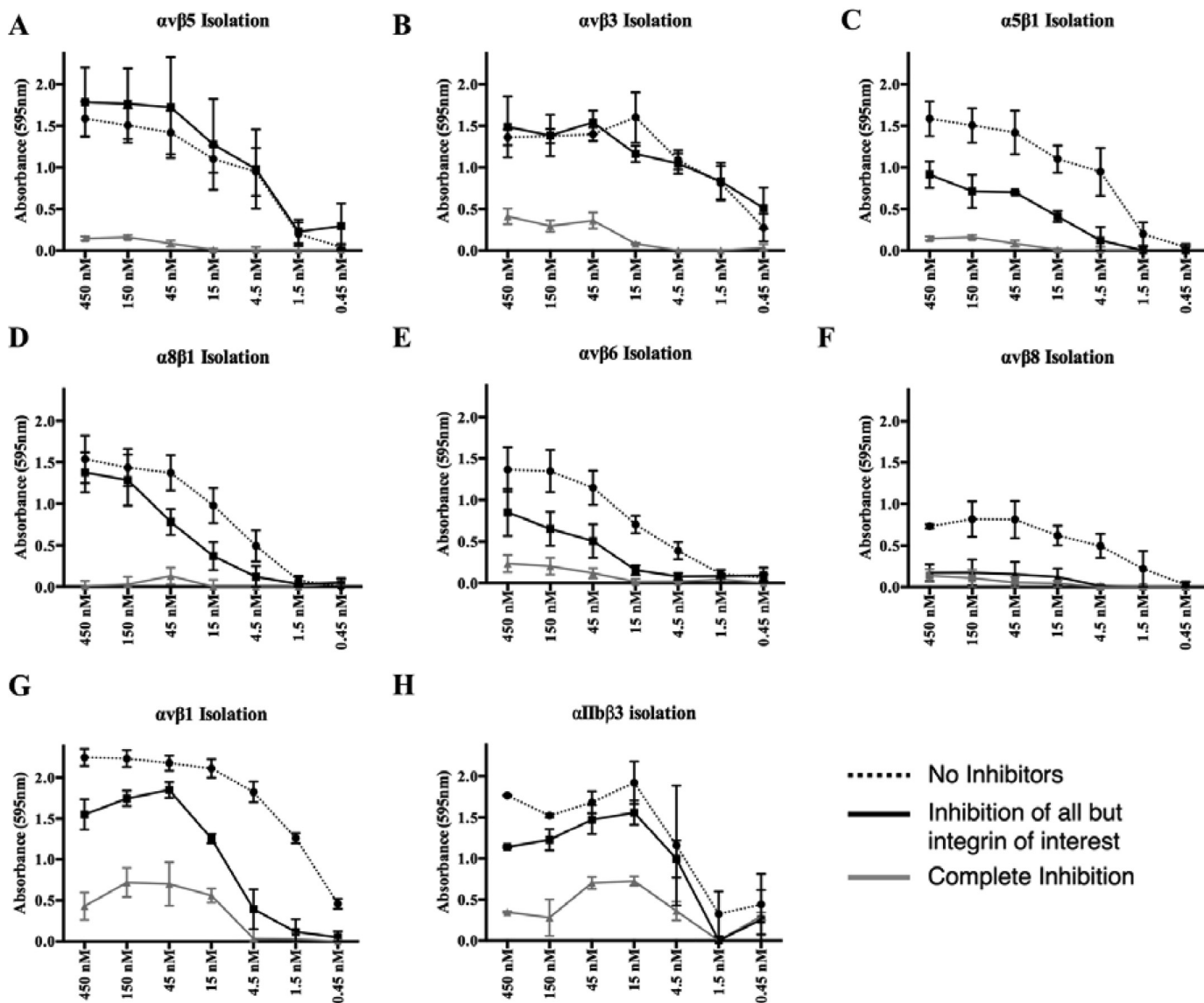
Figure 3. Binding capacities of the RGD-integrin family to WT fibrillin-1. For all panels, *x* axis denotes concentration of purified WT fibrillin-1. *A*, cell adhesion of integrin αvβ5 in SW480 cells, completed in the presence of P1D6. *B*, cell adhesion of integrin αvβ3 in SW480 cells transfected with integrin β3, completed in the presence of P1D6 and ALULA. *C*, cell adhesion of integrin α5β1 in SW480 cells, completed in the presence of ALULA. *D*, cell adhesion of integrin α8β1 in SW480 cells transfected with integrin α8, completed in the presence of P1D6 and ALULA. *E*, cell adhesion of integrin αvβ6 in SW480 cells transfected with integrin β6, completed in the presence of P1D6 and ALULA. *F*, cell adhesion of integrin αvβ8 in SW480 cells transfected integrin β8, completed in the presence of P1D6, ALULA, and 3G9. *G*, cell adhesion of integrin αvβ1 in HDF, completed in the presence of P1D6, ALULA, and AXUM2. *H*, cell adhesion of integrin αIIbβ3 in human platelets isolated from whole blood, completed in the presence of L230 and P5D2. Data represents mean of 2 biological replicates $\pm$ S.E.

ASBMB

*J. Biol. Chem.* (2019) 294(48) 18232–18243 **18235**
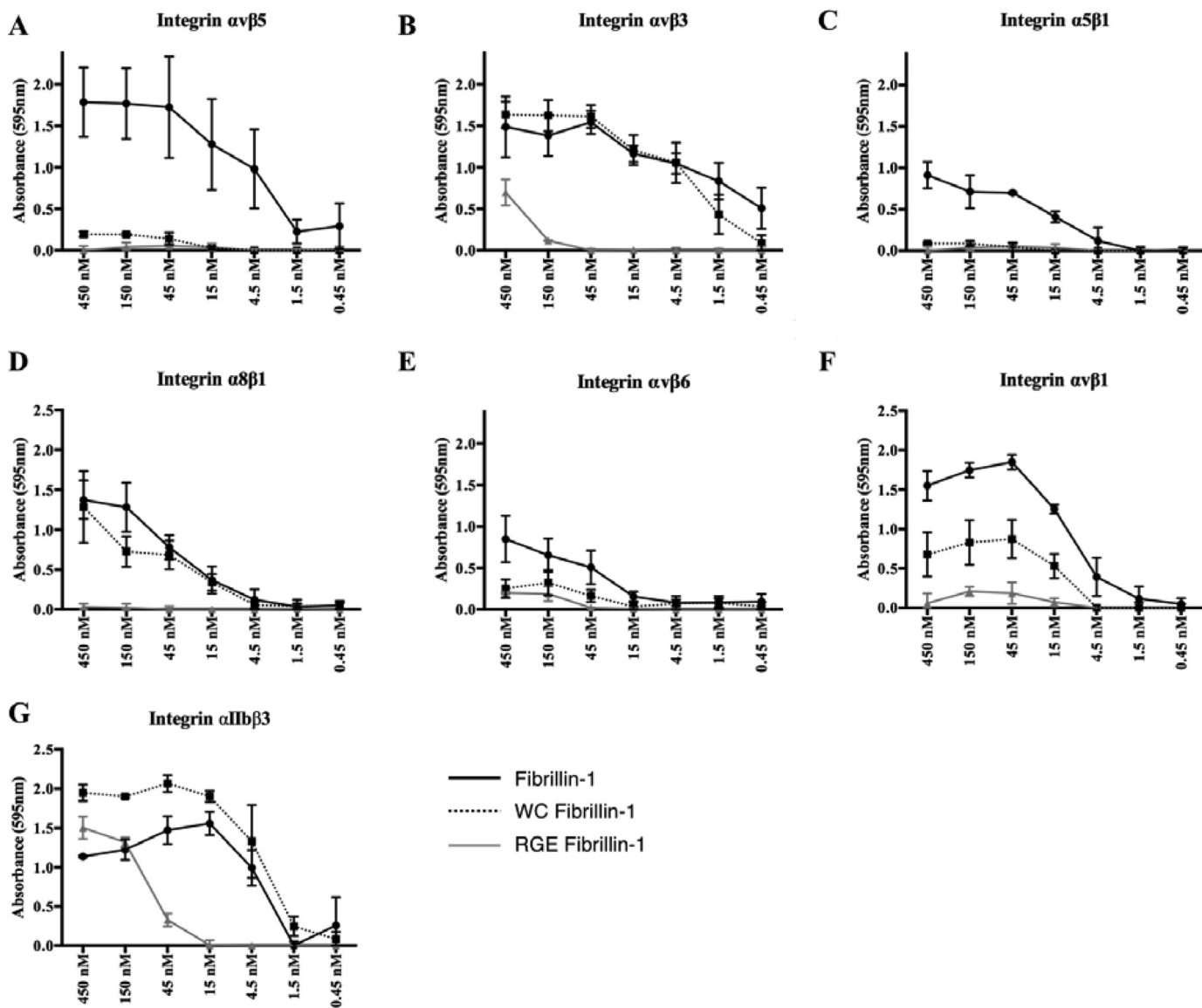
Figure 4. Binding capacities of the RGD-integrin family to the WT, disease causing (*WC*), and RGE knock-out fragments. For all panels, *x* axis denotes concentration of purified fibrillin-1 fragment. *A–E,* cell adhesion of endogenous and transfected integrins in SW480 cells. All conditions were completed in the presence of blocking antibodies against all integrins but one of interest. *F,* cell adhesion of integrin αvβ1 in HDF, completed in the presence of P1D6, ALULA, and AXUM2. *H,* cell adhesion of integrin αIIbβ3 in human platelets isolated from whole blood, completed in the presence of L230 and P5D2. Data represents mean of 2 biological replicates ± S.E.

pleted using HDF in the presence of blocking antibodies against αvβ3 (AXUM2), αvβ5, and α5β1. The contribution of αIIbβ3 was evaluated using human platelets in the presence of pan-specific αv and β1-blocking antibodies. Both cell types bound well to WT fibrillin-1 in the absence of blocking antibodies. Isolation studies with blocking antibodies allowed us to demonstrate that αvβ1 and αIIbβ3 are also highly effective integrin receptors for fibrillin-1 (Fig. 3, *G* and *H*), bringing the total number of integrins that can mediate adhesion to fibrillin-1 to 7. We confirmed that the addition of blocking antibodies specific to the isolated integrin markedly reduced adhesion in every case, demonstrating the specificity of this assay system.

We next determined how the SSS disease causing substitution (W1570C) affected adhesion mediated by each of the 7 integrins identified above. As shown in Fig. 4, the disease-causing WC mutation virtually abolished adhesion mediated by

αvβ5, α5β1, and αvβ6, but had no effect on adhesion mediated by αvβ3 or α8β1 (Fig. 4, *A–E*). In contrast, mutation of the RGD sequence to RGE dramatically inhibited binding of each of these 5 fibrillin–binding integrins. The SSS (WC) mutation substantially inhibited binding of αvβ1 to fibrillin-1, but this inhibition was not complete with adhesion mediated to the WC mutant at an intermediate level between WT fibrillin-1 and the RGE mutant (Fig. 4F). In contrast, the WC substitution did not inhibit binding mediated by integrin αIIbβ3. Rather, αIIbβ3-mediated adhesion was modestly increased by the WC mutation. As expected, the RGE mutation did substantially (albeit incompletely) inhibit αIIbβ3-mediated adhesion (Fig. 4G).

Taken together, these results suggest that the effects on integrin-binding of the disease-causing WC mutation in fibrillin-1 are not uniform across integrin heterodimers. Although 7 different integrins can bind to the RGD sequence in fibrillin-1
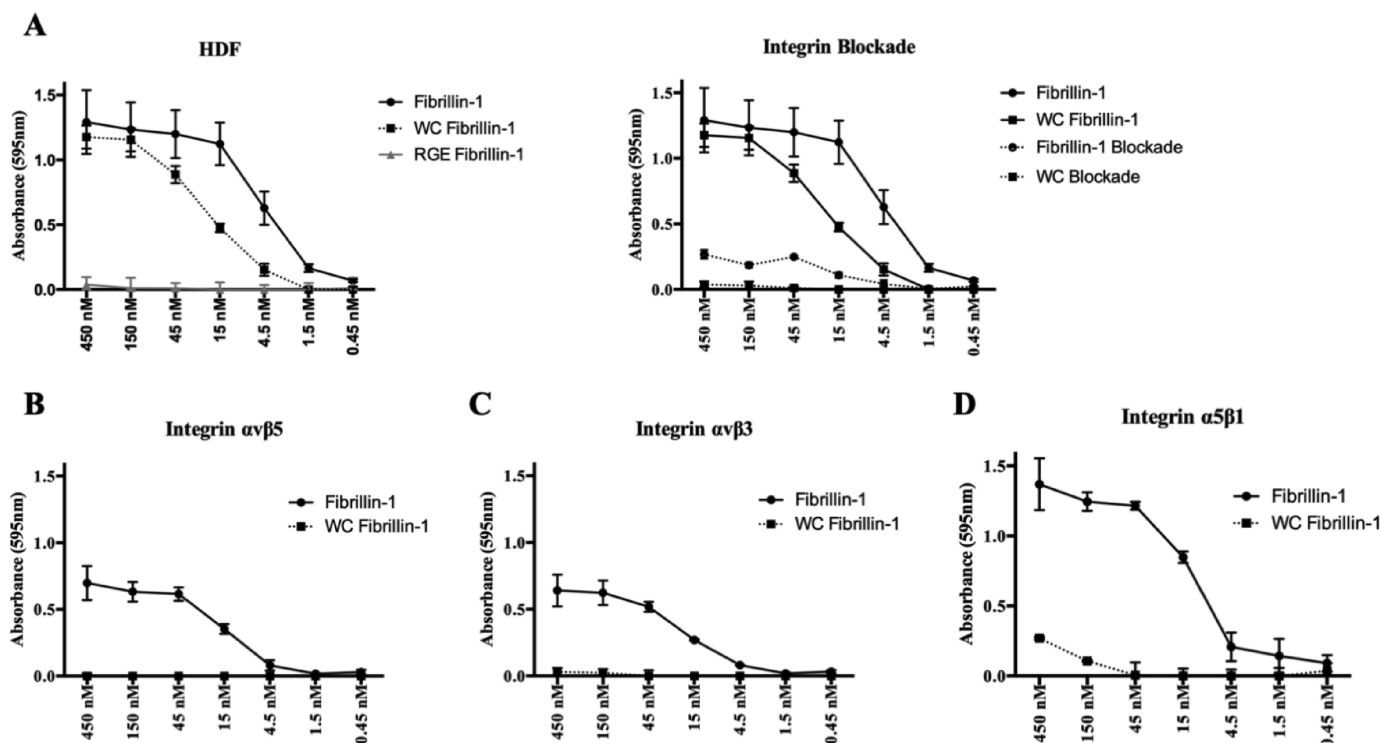
Figure 5. Binding capacities of the cell-surface integrins expressed in HDF cells to fibrillin-1 fragments. For all panels, *x* axis denotes the concentration of purified fibrillin-1 fragment. *A, left panel* indicates cell adhesion levels of HDF cells in the absence of treatment to all three fibrillin-1 fragments: WT, disease-causing mutant and RGE knockout. *Right panel* indicates complete integrin blockade of all relevant integrins using ALULA, PID6, AXUM2, and C8. *Solid line* denotes adhesion of HDF cells in the absence of antibody treatments; *dotted line* indicates integrin blockade for cells plated on the specified fragment. *B,* cell adhesion of integrin $\alpha v \beta 5$ in HDF cells, completed in the presence of P1D6, AXUM2, and compound C8. *C,* cell adhesion of integrin $\alpha v \beta 3$ in HDF cells, completed in the presence of ALULA, P1D6, and compound C8. *D,* cell adhesion of integrin $\alpha 5 \beta 1$ in HDF cells, completed in the presence of ALULA, AXUM2, and C8. Negative data for integrin binding to the RGE knockout is not indicated in *panels B–D*. Data represents mean of 2 biological replicates ± S.E.

(including 4 that have not been previously identified as fibrillin-1 receptors), only 3 of them, $\alpha v \beta 5$, $\alpha 5 \beta 1$, and $\alpha v \beta 1$, demonstrate binding that is substantially inhibited by the WC mutation.

HDF mediate adhesion to disease-causing fibrillin-1

To further understand the role of the RGD-integrin binding family in the progression of SSS, we used HDFs to assess whether or not the binding capacities determined in the SW480 transfection system were biologically relevant. HDF cells endogenously express $\alpha v \beta 1$, $\alpha v \beta 5$, $\alpha v \beta 3$, and $\alpha 5 \beta 1$ (Fig. 2, *D and E*). Using the cell-adhesion assay system previously described, we were surprised to find notable differences between the binding capacities of integrins expressed on the cell surface of HDFs and the SW480 system. The dermal cell line in the absence of antibody blocking treatment bound to both WT and the disease-causing mutant, although its adhesion to the mutant fragment was not as robust. Assays completed in the presence of the RGE-loss of integrin binding control showed no adhesion as expected. Adhesion was also abrogated for cells plated on fibrillin-1 and the disease-causing mutant in the presence of blocking reagents to all four integrins, confirming that HDF adhere to fibrillin-1 specifically through integrin interactions (Fig. 5*A*). The binding capacity of individual integrins was determined by a combination of specific integrin antibodies and C8, a small molecule inhibitor of integrin $\alpha v \beta 1$ (Table 1). In addition to $\alpha v \beta 1$, we found that integrins $\alpha v \beta 5$, $\alpha v \beta 3$, and $\alpha 5 \beta 1$ all mediated adhesion to the WT frag-

ment as identified with SW480s (Fig. 5, *B–D*). However, whereas $\alpha v \beta 3$ and $\alpha v \beta 5$ mediated very strong adhesion to fibrillin-1 in SW480 cells (Fig. 4, *A and B*), those binding capacities were not reflected in HDFs (Fig. 5, *B and C*). Rather, $\alpha 5 \beta 1$ (Fig. 5*D*) and $\alpha v \beta 1$ (Fig. 4*F*) showed the most robust binding profile to fibrillin-1 in the HDF cell line.

Adhesion assays completed on the disease-causing mutant (WC) confirmed that both $\alpha 5 \beta 1$ and $\alpha v \beta 5$ are unable to mediate cell adhesion to the mutant fragment (Fig. 5, *B and D*). In contrast to the binding profile observed with SW480s, integrin $\alpha v \beta 3$ showed complete loss of adhesion in HDFs (Fig. 5*C*). We theorized that this discrepancy may be due to the relative difference in cell-surface expression of $\alpha v \beta 3$ in the two cell lines (Fig. 2, *B and D*), as the SW480 over-expression system was designed to introduce a high copy number of the transfected integrin subunit. To validate the idea that local concentrations of integrin and ligand can have significant effects on adhesion, we completed additional adhesion assays with the overexpressed SW480-$\beta 3$ cell line using low concentrations of fibrillin and the disease-causing mutant. When integrin and ligand are present at high concentrations, $\alpha v \beta 3$ appears to bind to the WC mutant fragment with nearly as much affinity as fibrillin-1 (Fig. 4*B*). However, the separation between the binding profiles becomes apparent at ligand concentrations of 5 nM or less, suggesting that these interactions are highly dependent on the local stoichiometry of integrin and ligand, a factor that likely plays a vital role in the progression of SSS (Fig. S1). Although the

SW480 assay system clearly identified which members of the RGD-integrin binding family can recognize the RGD motif in fibrillin-1, the differences in integrin binding observed with HDFs suggests that the interactions between fibrillin-1 and the integrin family are regulated by factors other than binding affinity alone.

SSS fibrillin-1 mutant contains a free sulfhydryl

The TB4 domain of fibrillin-1 is characterized by an eight-cysteine motif that forms four disulfide bridges responsible for stabilizing the protein-fold (Fig. 6A). The hydrophobic core of this domain is further stabilized by the presence of tryptophan at position 1570, a feature that is conserved in all TB domains in fibrillins and LTBPs. In the SSS mutant this conserved tryptophan, which in the WT structure is within the range of three disulfide bonds (Fig. 6B), is replaced with a cysteine. In the WT structure, the Cβ atom of the Trp-1570 residue is within 5 Å of both Cys-1534 and Cys-1562. This is within the Cβ–Cβ distance seen in disulfide bonds in proteins (26). To determine whether the free sulfhydryl remained free or induced dimerization of the mutant fragment, we measured the concentration of protein sulfhydryls using Ellman's protocol. Ellman's reagent was replaced with 4,4′-dithiodipyridine (DTDP), an alternative reagent whose small size and amphiphilic nature allow it to react quickly with poorly accessible residues (27). DTDP was reacted with the WT and mutant fragment of fibrillin-1 at a range of protein concentrations, from which a concentration of SH was determined. The slope of the resulting plot denotes the number of free sulfhydryls within a protein fragment. The low value of WT fibrillin-1 confirms that all the cysteine residues in the protein fragment are sequestered in disulfide bonds (Fig. 6C). The SSS mutant, however, showed an increased slope close to the value of 1, suggesting that the mutant maintains a single free sulfhydryl without forming protein dimers. We further confirmed this observation by labeling the two proteins fragments with Alexa Fluor™ 647 C$_2$ maleimide, a fluorescent dye that reacts specifically with thiol groups (Fig. 6D) and by Coomassie staining the fragments in reduced *versus* nonreduced conditions (Fig. 6E). Reaction of the mutant fibrillin-1 fragment with the fluorescent dye confirmed the presence of an additional free cysteine residue, whereas the Coomassie staining demonstrated that both fragments remain monomers in solution.

The cell adhesion data strongly suggest that the SSS mutation does not simply eliminate integrin interactions with the RGD sequence in the TB4 domain. Introduction of a free sulfhydryl does not cause the protein to dimerize but instead induces a subtle change in the conformation of the RGD site that specifically, and differentially, mitigates interaction with only a subset of fibrillin-1– binding integrins.

Discussion

The results of this study show that 7 of the 8 RGD-binding integrins can mediate cell adhesion to WT fibrillin-1. Four of these, $\alpha8\beta1$, $\alpha v\beta1$, $\alpha v\beta5$, and $\alpha IIb\beta3$, have not been previously described as receptors for fibrillin-1. Mutation of the RGD sequence in the fourth TB domain to RGE abrogated adhesion mediated by 6 of these integrins ($\alpha5\beta1$, $\alpha8\beta1$, $\alpha v\beta1$, $\alpha v\beta3$,

$\alpha v\beta5$, and $\alpha v\beta6$) and substantially inhibited adhesion mediated by $\alpha IIb\beta3$, confirming that cell adhesion was mediated by direct interaction of each of these integrins with the RGD site. In contrast to the RGE mutation, the tryptophan to cysteine missense mutation responsible for causing SSS differentially affected binding of these integrins to fibrillin-1. Adhesion mediated by $\alpha5\beta1$, $\alpha v\beta5$, and $\alpha v\beta6$, at the levels expressed on the respective cell lines, was entirely abrogated by the disease-causing mutation and adhesion mediated by $\alpha v\beta1$ was partially abrogated. In contrast, adhesion mediated by $\alpha8\beta1$ and $\alpha IIb\beta3$ was either unaffected or modestly enhanced (in the case of $\alpha IIb\beta3$). Adhesion to the disease-causing mutant mediated by integrin $\alpha v\beta3$ was highly dependent on cell-surface expression of the integrin.

Progression of SSS has been studied extensively by histologic evaluation of the dermis of affected patients. Immunohisto-chemistry of skin biopsies suggests that dermal fibroblasts are responsible for the increase in collagen that is observed in patients (12). The adhesion assays completed in human dermal fibroblasts allowed us to use a biologically relevant cell line to evaluate the integrins that could play a role in disease progression, namely $\alpha v\beta3$, $\alpha v\beta5$, $\alpha5\beta1$, and $\alpha v\beta1$. Although integrins $\alpha v\beta5$ and $\alpha5\beta1$ behaved similarly in both HDF and SW480 cell lines, $\alpha v\beta3$ showed robust binding to the mutant fragment in the transfected SW480 cells that was not observed in HDFs. Although surprising, this discrepancy suggests that the local concentration of integrin and ligand plays a critical role in how cells respond to the disease-causing mutation in fibrillin-1. The effect was emphasized by the finding that in SW480 cells over-expressing $\beta3$, adhesion to the WT fragment persists at low nanomolar concentrations, whereas adhesion to the mutant fragment begins to diminish significantly. This difference suggests that in the presence of the Trp to Cys mutation, binding of the RGD-integrin subfamily can be altered by the local stoichiometry of the two binding partners.

A similar observation was also made for $\alpha v\beta5$ and $\alpha5\beta1$. Although the relative binding capacities to WT and mutant fragments were mirrored in both cell lines, they showed substantial differences in absolute affinity for adhesion. Integrin $\alpha v\beta5$ is a strong mediator of adhesion to fibrillin-1 in SW480 cells, whereas in HDF $\alpha5\beta1$ is observed as the dominant fibrillin-1– binding partner. Given the higher cell-surface expression of integrin $\alpha5\beta1$ in HDFs, this result is understandable. The differences observed between these two cell lines further highlights the importance of gaining a clearer understanding of the local cellular and matrix composition of the dermis in SSS.

As noted earlier, mice expressing either a knock-in of a cysteine for tryptophan substitution in mouse fibrillin-1, at the same location as the human disease-causing WC mutation, or a knock-in of a glutamic acid for aspartic acid substitution in the exposed RGD site (RGE), both cause skin thickening reminiscent of stiff skin syndrome (14). These results strongly support the hypothesis that SSS is due, at least in part, to loss of integrin binding to mutant fibrillin-1. Our results using the HDF cell line suggest that integrins $\alpha5\beta1$, $\alpha v\beta3$, $\alpha v\beta5$, and $\alpha v\beta1$ play relevant roles in disease progression. The remaining members of the RGD-binding integrin subfamily were not inhibited by

A

B

C

	Linear Slope
Fibrillin-1	0.1849
SSS Mutant	0.7479

D

E
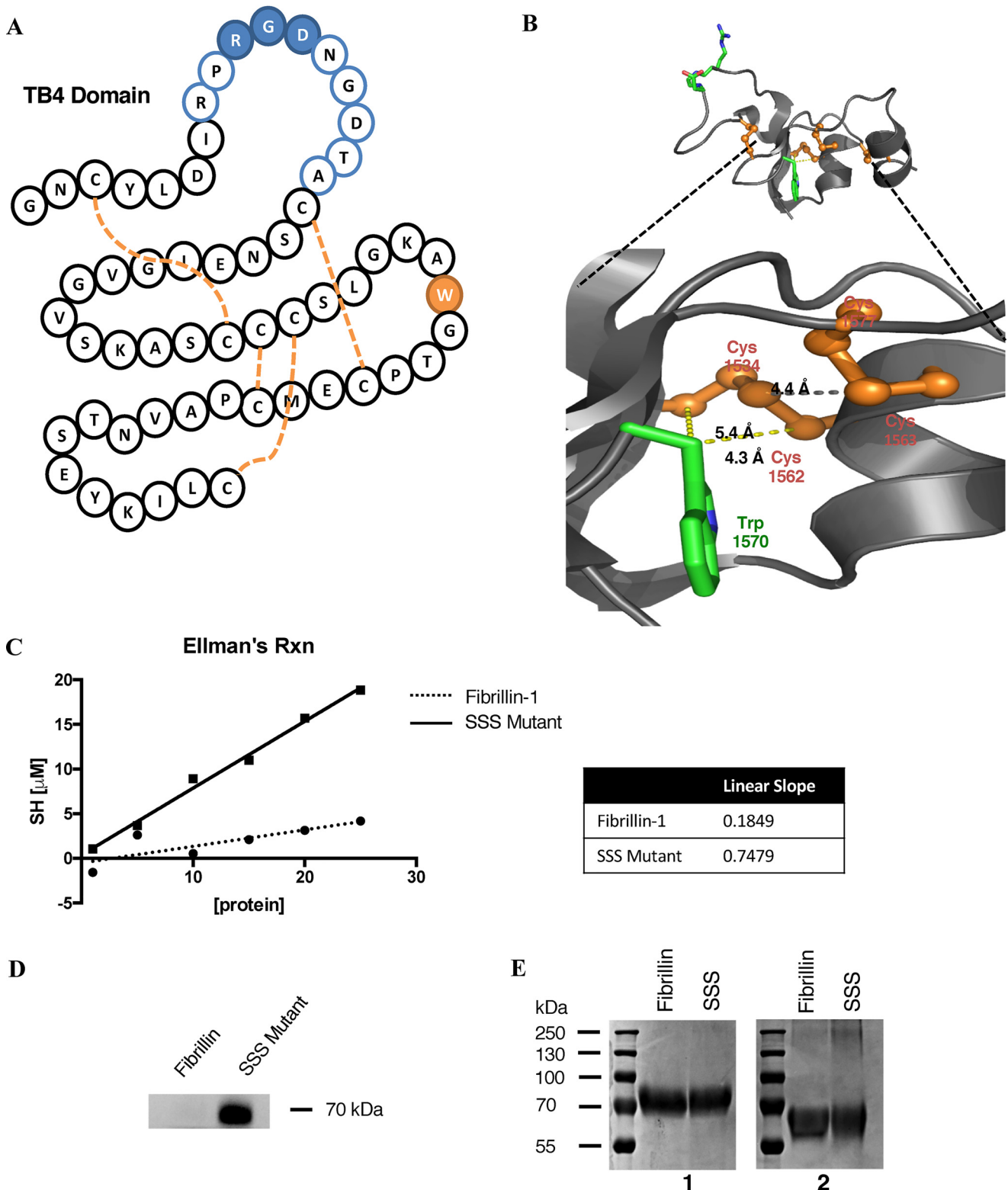
Figure 6. *A,* schematic of the TB4 domain in fibrillin-1. The flexible RGD loop is denoted in *blue,* tryptophan 1570 in *green,* and the disulfide bridges by *dashed orange lines. B,* tertiary structure of TB4 from the crystalized fragment (17). Amino acid 1570 is shown in the WT construct as tryptophan (*green*) and surrounding cysteines in *orange. C,* Ellman's reaction completed using 4,4′-dithiodipyridine reagent on a serial dilution of WT and mutant fibrillin-1. Absorbance measurements were done in 1-cm cuvettes. *D,* fluorescent labeling of WT and mutant fibrillin-1 fragments using Alexa Fluor™ 647 C$_2$ maleimide, the labeled protein was run on a 4–10% SDS-PAGE, and imaged using the 650-nm laser line. *E,* Coomassie staining of reduced (*1*) *versus* nonreduced (*2*) samples run on an 8% SDS-PAGE.

the WC mutation in fibrillin-1, suggesting that their endogenous roles are unaffected in this disease background. Integrin αvβ1 did show partial loss of binding, potentially explaining

why the HDF cells are able to maintain adhesion to the mutant fragment. Notably, the binding profile of αvβ1 to the mutant fragment does not mirror the strong adhesion observed in HDFs

plated on the disease-causing mutant. Although our data support the idea that adhesion of HDFs to WC fibrillin-1 is an integrin-dependent interaction, our data does not clearly identify which integrin expressed on HDF cells mediates that binding interaction.

It has been suggested that cells plated on the mutant fragment show a different cell-surface expression profile for several relevant integrins (15). Increases in active $\alpha v\beta 3$ and $\alpha 5\beta 1$ have also been observed through studies of the Fbn1$^{W1572C/+}$ mouse model. These differences were observed in dermal cell lines as well as infiltrating dendritic cells, suggesting that the composition of the local matrix directly affects how integrins are expressed and recruited to the cell surface. The binding of HDFs to mutant fibrillin-1 reflect the possibility that a more complex signaling pattern exists between mutant fibrilln-1 and the cells plated on its surface. The work completed in the knockout SSS mouse model by Gerber *et al.* (15) also suggested that $\beta 1$ activation and $\alpha v\beta 3$ blockade may play important roles in disease progression. Our findings that both $\alpha 5\beta 1$ and $\alpha v\beta 1$ show significant loss of binding to the mutant fragment support the role of $\beta 1$ integrins in this disease process. Furthermore, our observation that integrin $\alpha v\beta 3$ is only capable of mediating adhesion to the mutant fragment at high cell-surface expression levels is in concordance with the finding that Fbn1$^{W1572C/+}$ mice bred with haploinsufficient $\beta 3$ knockout mice showed protection from progression of SSS (15). Taken together, these results suggest that $\alpha v\beta 3$ may be a potential therapeutic target for this disease process, although we cannot exclude indirect roles for other integrins in the more complex *in vivo* environment of the skin.

In WT fibrillin-1, the fragment used for cell-adhesion assays contains an even number of cysteine residues that are all included in disulfide bonds, leaving no free sulfhydryls, as confirmed by fluorescent labeling and DTDP reactivity. In the absence of extensive secondary structure and an extended hydrophobic core, the individual domains of fibrillin-1 rely on a large number of disulfides for structural stability. The mutation of a highly conserved tryptophan to cysteine within the RGD-containing TB4 domain could easily prompt disulfide shuffling given its key role in stabilizing the hydrophobic core of this domain. Furthermore, this large hydrophobic residue (Trp-1570) also plays a prominent role in packing against adjacent disulfide bonds, and hence in stabilizing their pairing. The WC mutation removes the tryptophan that forms the hydrophobic core of domain TB4 and replaces it with an additional cysteine, which could remain as a free sulfhydryl, initiate dimerization of the fragment, or cause a misfold with a free thiol that is inaccessible. Coomassie staining of the mutant in nonreduced conditions as well as reactivity with DTDP, confirmed the presence of a single cysteine that remained free but did not result in protein dimerization. Because the 8-cysteine motif of TB4 is responsible for stabilizing the globular structure of this domain, the addition of a new cysteine residue at position 1570 has the potential to change the stability of the mutant fragment by causing the reshuffling of disulfide bonds and creating a free sulfhydryl at a separate location. In either case, this mutation is likely to cause a significant change in the conformation of the TB4 domain, affecting the structural context of the exposed RGD site.

Rearrangements in the internal conformation of this domain would lead to alterations in tertiary structure, which would be expected to influence the specificity and affinity of RGD-binding integrins for this domain. Although these integrins interact with the local RGD site, it is well-known that different RGD-binding integrins preferentially interact with RGD sites depending on the surrounding sequences and on the secondary and tertiary structures of ECM proteins (28, 29).

A functional RGD sequence is defined by a flexible loop that allows for a conformation in which the side chains of the tripeptide are pointed out in almost opposite directions (30, 31). The outward extension of the motif allows for ease of accessibility by RGD-binding receptors; tertiary or quaternary structures that result in the burial of the RGD sequence will not interact with the integrin-binding pocket. Furthermore, the amino acids flanking the C terminus of the RGD-domain have been shown to have a significant effect on the ability to mediate robust integrin binding. Peptides containing glycine, tryptophan, or phenylalanine following the RGD motif are easily recognized by $\alpha 5\beta 1$ (32). Substitution of serine or alanine in those sites results in preferential binding by $\alpha v\beta 3$ and $\alpha v\beta 5$. An even more specific peptide containing tyrosine or arginine results in highly potent recognition by $\alpha IIb\beta 3$ (33). Not only is the immediate flanking sequence of the RGD motif important for integrin binding, the positioning of a ligand's secondary structure can also have a dramatic effect. For example, integrins $\alpha 5\beta 1$ and $\alpha v\beta 3$ are both known receptors for mediating cell adhesion to fibronectin (FN). Although $\alpha v\beta 3$ recognizes the RGD motif in the 10th type III repeating unit of FN, $\alpha 5\beta 1$ requires a synergy site in the 9th type III unit, PHSRN (34). Absence of this amino acid sequence results in a substantial loss of binding by $\alpha 5\beta 1$ but does not affect the binding capacity of $\alpha v\beta 3$. These differences in recognition demonstrates the importance of FN topology for receptor binding to the RGD site (35, 36). Fibrillin binding to $\alpha v\beta 3$ and $\alpha v\beta 6$ has also been shown to be dependent on domain context. $\alpha v\beta 3$ requires cbEGF22 together with TB4 to achieve high affinity binding, whereas $\alpha v\beta 6$ does not (37).

Although the RGD site of fibrillin-1 is 20 Å removed from the mutated tryptophan 1570 site in the WT structure, it is reasonable to expect the W1570C mutation to influence integrin specificity by both altering the local conformational energy and dynamics of its RGD tripeptide as well as more distant interactions. Our results further demonstrate the importance of the secondary and tertiary structures in ligand-binding interactions for the RGD-integrin subfamily. The cell-adhesion assays demonstrate that the WC mutant of fibrillin-1 does not simply abrogate binding of the 7 fibrillin-1 integrins. Our data shed light on how the WC mutation in fibrillin-1 could abrogate interaction with a specific subset of integrins, which is presumably the first step in the initiation of the cutaneous pathology that characterizes this disease.

Experimental procedures

Reagents

Purified mouse anti-CD51 (integrin αv) was purchased from BD Biosciences; rabbit anti-integrin $\beta 1$ was purchased from Millipore; ChromePure mouse IgG was purchased from Jack-

Clone	Source	Integrin specificity
L230	ATTC Hybridoma	αV
P5D2	Developmental Studies Hybridoma Bank	$\beta 1$
P1D6	Fred Hutchinson Cancer Center	$\alpha 5\beta 1$
ALULA	Sheppard Lab	$\beta 5$
AXUM2	Sheppard Lab	$\beta 3$
ADWA-11	Sheppard Lab	$\beta 8$
3G9	Biogen	$\beta 6$
10E5	Rockefeller University	$\alpha IIb\beta 3$
YZ83	Hiroshima University	$\alpha 8\beta 1$

son ImmunoResearch. Anti-αv mouse mAb, L230 (38), was purified in our lab from a hybridoma obtained from ATCC. Anti-$\beta 1$ mouse mAb, P5D2, was purified in our lab from a hybridoma obtained from DSHB. Anti-$\alpha 5\beta 1$ mouse mAb P1D6 was a generous gift from Elizabeth Wayner (Fred Hutchinson Cancer Center). Anti-$\alpha IIb\beta 3$ mouse mAb 10E5 was a generous gift from Barry S. Coller (Rockefeller University). Anti-$\alpha 8\beta 1$ mouse mAb YZ83 was a generous gift from Yasuyuki Yokosaki (Hiroshima University). Mouse monoclonal antibodies against $\alpha v\beta 5$ (ALULA), $\alpha v\beta 3$ (AXUM2), and $\alpha v\beta 8$ (ADWA-11) were generated in our laboratory and anti-$\alpha v\beta 6$ mouse mAb 3G9 was a generous gift from Biogen Inc. (Table 2). 4,4′-Dithio-dipyridine was purchased from Sigma-Aldrich and Alexa-Fluor^{TM} 647 C_2 maleimide was purchased from Invitrogen. Compound C8 is a small molecule inhibitor of integrin $\alpha v\beta 1$, and was synthesized by Dr. Hyunil Jo, Department of Pharmaceutical Chemistry at UCSF, and resuspended in 50% dimethyl sulfoxide.

Cells

HDF and growth kit medium were purchased from ATCC and cultured according to the vendor's instructions. Colon carcinoma SW480 cells were used to generate transfected cell lines that overexpressed integrin subunits, $\alpha 8$, $\beta 3$, $\beta 6$, and $\beta 8$, as previously described.

Isolation of human platelets

Whole blood was drawn using a plastic syringe containing 1/10 volume CPD buffer (15 mM citric acid, 90 mM sodium citric, 16 mM $Na_2H_2PO_4$, 142 mM D-glucose, pH 7.4) with 1 μM prostaglandin E1. Cells were mixed gently, transferred to a 50-ml conical and spun at $200 \times g$ for 15 min at room temperature. The top layer containing the platelet-rich plasma was transferred to a new 15-ml conical containing 1/10 volume of buffer ACD (39 mM citric acid, 75 mM sodium citric, 135 mM D-glucose, pH 7.4). Prostaglandin E1 was added to a final concentration of 0.4 μg/ml to prevent platelet activation. Cells were pelleted by centrifugation at $800 \times g$ for 20 min at room temperature. Platelets were rinsed with wash buffer (10 mM sodium citric, 150 mM NaCl, 1 mM EDTA, 1% D-glucose, pH 7.4) without resuspension to avoid unnecessary activation. Cells were carefully resuspended in 5–10 ml of HEPES-Tyrodes's buffer (134 mM NaCl, 12 mM $NaHCO_3$, 2.9 mM KCl, 0.34 mM dibasic Na_2HPO_4, 1 mM $MgCl_2$, 1 mM $CaCl_2$, 10 mM HEPES, 5 mM glucose, 1% BSA, pH 7.4). For use in adhesion assays, platelets were activated using PAR-1 at a final concentration of 100 μM.

Immunoprecipitation

HDF and SW480 cells were lysed in 50 mM Tris-HCl, pH 7.5, 10 mM $MgCl_2$, 150 mM NaCl, and 1% Triton X-100, with protease and phosphatase inhibitor mixture (Thermo Scientific). Lysates were centrifuged and total protein concentration was determined using Pierce BCA Protein Assay Kit. Samples were incubated with integrin αv antibody L230 for 1 h at 4 °C with rotation (70 rpm). Protein G-Sepharose (GE Healthcare) beads were then added with a further 1-h incubation. Samples were washed four times with 1 ml of lysis buffer and eluted with reducing sample buffer, resolved by SDS-PAGE, and analyzed by immunoblot.

Flow cytometry

HDF and SW480 cells were collected from 10-cm dishes with 0.05% trypsin-EDTA and washed twice with PBS. 1×10^6 cells were re-suspended in PBS supplemented with 1% BSA and then incubated with primary antibody at 4 °C for 1 h. Cells were washed twice with PBS before incubation with secondary antibody conjugated to phycoerythrin (PE; Jackson Immuno-Research). Cells were washed twice with PBS before analysis on a BD FACSCantoII. Antibodies were used at a final concentration of 1 μg/ml as follows: anti-integrin $\beta 3$ (AXUM2), anti-integrin $\beta 6$ (3G9), anti-integrin $\beta 5$ (ALULA), and anti-integrin αv (L230). A chicken anti-integrin $\alpha 8$ (YZ83) antibody was used at 2 μg/ml (generous gift from Dr. Yasuyuki Yokasaki) and anti-integrin $\alpha 5$ (P1D6) was used at 1 μg/ml.

Cell-adhesion assay

96-Well flat-bottomed Immulon 4HBX microtiter plates (Thermo Scientific) were coated with a series of fibrillin-1 protein concentrations diluted in DPBS and then incubated at 37 °C for 1 h. Wells were washed with DPBS before blocking with 2% BSA prepared in DPBS at 37 °C for 1 h. Cells were detached from confluent 10-cm dishes using 0.05% trypsin-EDTA and re-suspended in serum-free Dulbecco's modified Eagle's medium. Wells were plated with 5×10^4 cells. For blocking conditions, cells were incubated with 10 μg/ml of the indicated antibody or 10 μM C8 (Table 1) for 10 min at 4 °C before final plating. Plates were centrifuged at 300 rpm for 5 min prior to a 1-h incubation at 37 °C in a 5% CO_2 humidified incubator. Nonadherent cells were removed by centrifugation (top side down) at 500 rpm for 5 min. Remaining adhered cells were stained with 0.5% crystal violet, 0.1% formaldehyde and wells were subsequently washed with PBS. The relative number of cells in each well was determined after solubilization in 40 μl of 2% Triton X-100, absorbance was read at 595 nm in a microplate reader (Bio-Rad Laboratories). All determinations were carried out in triplicate.

Expression and protein purification

The pSecTag2A plasmids containing cbEGF19–cbEGF25 of WT fibrillin-1 and the disease-causing mutation (WC) were generously provided by Dr. Penny A. Handford. Mutagenesis of

this plasmid was completed using QuikChange Site-directed Mutagenesis Kit to generate the RGE fibrillin-1 fragment. Nucleotide 1543 was mutated to generate a Asp to Glu substitution. All three protein fragments contained a His tag for purification on the C terminus and were expressed in HEK293FS cells; a 1-liter volume of 1×10^9 cells were transfected using 1 mg of DNA (293Fectin™, Thermo Scientific). Cells were allowed to grow for 5 days before medium was collected and diluted 3-fold in 50 mM Tris, pH 8, 200 mM NaCl (resuspension buffer) in a Schott bottle. Ni^{2+}-charged chelating Sepharose beads (ThermoScientific) were prepped in resuspension buffer before adding to diluted medium and incubated at 4 °C for 4 h with gentle shaking. Sepharose beads were packed into a 10-ml column and washed with 50 ml of cold wash buffer (10 mM imidazole, 50 mM Tris, pH 8, 200 mM NaCl). Protein was eluted with 20 ml of cold elution buffer (300 mM imidazole, 50 mM Tris, pH 8.0, 200 mM NaCl). 1-ml fractions were collected and run on 10% SDS-PAGE to determine elution of protein. Fractions were dialyzed at 4 °C into resuspension buffer using a Slide-A-Lyzer Dialysis Cassette (Pierce). Final protein concentration was determined using a BCA Protein Assay Kit (Pierce) and fragments were stored at 4 °C in 0.1% sodium azide.

Quantification of protein thiols with DTDP

Protein samples were adjusted to a volume of 250 μl in DPBS containing 2% SDS and denatured for 15 min. Samples were added to 2.5 ml of reaction buffer (100 mM NaH$_2$PO$_4$, 1 mM EDTA, pH 8). Samples were vortexed and incubated at room temperature for 5 min after the addition of 50 μl of 4 mM DTDP. Absorbance at 324 nm was read against a water blank (1 cm light path). Absorbance values were corrected using an additional DTDP blank. The amount of free sulfhydryl from solution in the spectrophotometric cuvette was calculated according to $E = (A)/bc$, where A = absorbance, b = path length in centimeters, and c = concentration in moles/liter of SH. The molar extinction coefficient for DTDP in this buffer system is 21,400 M^{-1} cm^{-1}. Final concentrations were determined by adjusting for the dilution factor of the 2.8-ml reaction volume.

Fluorescent labeling with Alexa Fluor™ 647 C$_2$ maleimide

Protein samples were diluted to 0.2 mg/ml in 100 mM Tris-HCl, pH 7. Alexa Fluor™ 647 C$_2$ maleimide was added to a final concentration of 0.5 mM and samples were incubated in the dark at room temperature for 30–60 min. Labeled fragments were run on a 4–12% Tris glycine SDS-PAGE and imaged using the 650-laser line.

References

1. Sakai, L. Y., Keene, D. R., and Engvall, E. (1986) Fibrillin, a new 350-kDa glycoprotein, is a component of extracellular microfibrils. *J. Cell Biol.* **103,** 2499–2509 CrossRef Medline
2. Ramirez, F., and Dietz, H. C. (2007) Fibrillin-rich microfibrils: structural determinants of morphogenetic and homeostatic events. *J. Cell Physiol.* **213,** 326–330 CrossRef Medline
3. Jensen, S. A., Robertson, I. B., and Handford, P. A. (2012) Dissecting the fibrillin microfibril: structural insights into organization and function. *Structure* **20,** 215–225 CrossRef Medline
4. Dietz, H. C., Cutting, G. R., Pyeritz, R. E., Maslen, C. L., Sakai, L. Y., Corson, G. M., Puffenberger, E. G., Hamosh, A., Nanthakumar, E. J., and Curristin, S. M. (1991) Marfan syndrome caused by a recurrent *de novo* missense mutation in the fibrillin gene. *Nature* **352,** 337–339 CrossRef Medline
5. Lee, B., Godfrey, M., Vitale, E., Hori, H., Mattei, M. G., Sarfarazi, M., Tsipouras, P., Ramirez, F., and Hollister, D. W. (1991) Linkage of Marfan syndrome and a phenotypically related disorder to two different fibrillin genes. *Nature* **352,** 330–334 CrossRef Medline
6. Gupta, P. A., Putnam, E. A., Carmical, S. G., Kaitila, I., Steinmann, B., Child, A., Danesino, C., Metcalfe, K., Berry, S. A., Chen, E., Delorme, C. V., Thong, M. K., Adès, L. C., and Milewicz, D. M. (2002) Ten novel FBN2 mutations in congenital contractural arachnodactyly: delineation of the molecular pathogenesis and clinical phenotype. *Hum. Mutat.* **19,** 39–48 CrossRef Medline
7. Corson, G. M., Charbonneau, N. L., Keene, D. R., and Sakai, L. Y. (2004) Differential expression of fibrillin-3 adds to microfibril variety in human and avian, but not rodent, connective tissues. *Genomics* **83,** 461–472 Medline
8. Pereira, L., D'Alessio, M., Ramirez, F., Lynch, J. R., Sykes, B., Pangilinan, T., and Bonadio, J. (1993) Genomic organization of the sequence coding for fibrillin, the defective gene product in Marfan syndrome. *Hum. Mol. Genet.* **2,** 961–968 CrossRef Medline
9. Handford, P. A. (2000) Fibrillin-1, a calcium binding protein of extracellular matrix. *Biochim. Biophys. Acta* **1498,** 84–90 CrossRef Medline
10. Robertson, I., Jensen, S., and Handford, P. (2011) TB domain proteins: evolutionary insights into the multifaceted roles of fibrillins and LTBPS. *Biochem. J.* **433,** 263–276 CrossRef Medline
11. Yadin, D. A., Robertson, I. B., McNaught-Davis, J., Evans, P., Stoddart, D., Handford, P. A., Jensen, S. A., and Redfield, C. (2013) Structure of the fibrillin-1 N-terminal domains suggests that heparan sulfate regulates the early stages of microfibril assembly. *Structure* **21,** 1743–1756 CrossRef Medline
12. Loeys, B. L., Gerber, E. E., Riegert-Johnson, D., Iqbal, S., Whiteman, P., McConnell, V., Chillakuri, C. R., Macaya, D., Coucke, P. J., De Paepe, A., Judge, D. P., Wigley, F., Davis, E. C., Mardon, H. J., Handford, P., Keene, D. R., Sakai, L. Y., and Dietz, H. C. (2010) Mutations in fibrillin-1 cause congenital scleroderma: stiff skin syndrome. *Sci. Transl. Med.* **2,** 23ra20 Medline
13. Olivieri, J., Smaldone, S., and Ramirez, F. (2010) Fibrillin assemblies: extracellular determinants of tissue formation and fibrosis. *Fibrogenesis Tissue Repair.* **3,** 24 CrossRef Medline
14. Sakamoto, H., Broekelmann, T., Cheresh, D. A., Ramirez, F., Rosenbloom, J., and Mecham, R. P. (1996) Cell-type specific recognition of RGD- and non-RGD-containing cell binding domains in fibrillin-1. *J. Biol. Chem.* **271,** 4916–4922 CrossRef Medline
15. Gerber, E. E., Gallo, E. M., Fontana, S. C., Davis, E. C., Wigley, F. M., Huso, D. L., and Dietz, H. C. (2013) Integrin-modulating therapy prevents fibrosis and autoimmunity in mouse models of scleroderma. *Nature* **503,** 126–130 CrossRef Medline
16. Pfaff, M., Reinhardt, D. P., Sakai, L. Y., and Timpl, R. (1996) Cell adhesion and integrin binding to recombinant human fibrillin-1. *FEBS Lett.* **384,** 247–250 CrossRef Medline
17. Bax, D. V., Bernard, S. E., Lomas, A., Morgan, A., Humphries, M. J., Shuttleworth, C. A., and Kielty, C. M. (2003) Cell adhesion to fibrillin-1 molecules and microfibrils is mediated by α$_5$β$_1$ and α$_v$β$_3$ integrins. *J. Biol. Chem.* **278,** 34605–34616 CrossRef Medline

ASBMB

18. Lee, S. S., Knott, V., Jovanović, J., Harlos, K., Grimes, J. M., Choulier, L., Mardon, H. J., Stuart, D. I., and Handford, P. A. (2004) Structure of the integrin binding fragment from fibrillin-1 gives new insights into microfibril organization. *Structure* **12,** 717–729 CrossRef Medline

19. Jovanovic, J., Takagi, J., Choulier, L., Abrescia, N. G., Stuart, D. I., van der Merwe, P. A., Mardon, H. J., and Handford, P. A. (2007) αvβ6 is a novel receptor for human fibrillin-1: comparative studies of molecular determinants underlying integrin-RGD affinity and specificity. *J. Biol. Chem.* **282,** 6743–6751 CrossRef Medline

20. Hynes, R. O. (2002) Integrins: bidirectional, allosteric signaling machines. *Cell* **110,** 673–687 CrossRef Medline

21. Weinacker, A., Chen, A., Agrez, M., Cone, R. I., Nishimura, S., Wayner, E., Pytela, R., and Sheppard, D. (1994) Role of integrin αvβ6 in cell attachment to fibronectin: heterologous expression of intact and secreted forms of the receptor. *J. Biol. Chem.* **269,** 6940–6948 Medline

22. Yokosaki, Y., Monis, H., Chen, J., and Sheppard, D. (1996) Differential effects of the integrins α9β1, αvβ3 and αvβ6 on cell proliferative responsive to tenascin: roles of the β subunit extracellular and cytoplasmic domains. *J. Biol. Chem.* **271,** 24144–24150 CrossRef Medline

23. Schnapp, L. M., Hatch, N., Ramos, D. M., Klimanskaya, I. V., Sheppard, D., and Pytela, R. (1995) The human integrin α8β1 functions as a receptor for tenascin, fibronectin, and vitronectin. *J. Biol. Chem.* **270,** 23196–23202 CrossRef Medline

24. Jackson, T., Clark, S., Berryman, S., Burman, A., Cambier, S., Mu, D., Nishimura, S., and King, A. M. (2004) Integrin αvβ8 functions as a receptor for foot-and-mouth disease virus: role of the β-chain cytodomain in integrin-mediated infection. *J. Virol.* **78,** 4533–4540 CrossRef Medline

25. Wagner, C. L., Mascelli, M. A., Neblock, D. S., Weisman, H. F., Coller, B. S., and Jordan, R. E. (1996) Analysis of GPIIb/IIIa receptor number by quantification of 7E3 binding to human platelets. *Blood* **88,** 907–914 Medline

26. Richardson, J. S. (1981) The anatomy and taxonomy of protein structure. *Adv. Prot. Chem.* **34,** 167–339 Medline

27. Hansen, R. E., Østergarrd, H., Nørgaard, P., and Winther, J. R. (2007) Quantification of protein thiols and dithiols in the picomolar range using sodium borohydride and 4,4′-dithiodipyridine. *Anal. Biochem.* **363,** 77–82 CrossRef Medline

28. Hass, T. A., and Plow, E. F. (1994) Integrin-ligand interactions: a year in review. *Curr. Opin. Cell Biol.* **6,** 656–662 CrossRef

29. Ruoslahti, E. (1996) RGD and other recognition sequences for integrins. *Annu. Rev. Cell Dev. Biol.* **12,** 697–715 CrossRef Medline

30. Dickinson, C. D., Veerapandian, B., Dai, X. P., Hamlin, R. C., Xuong, N. H., Ruoslahti, E., and Ely, K. R. (1994) Crystal structure of the tenth type Ill cell adhesion module of human fibronectin. *J. Mol. Biol.* **236,** 1079–1092 CrossRef Medline

31. Krezel, A. M., Wagner, G., Seymour-Ulmer, J., and Lazarus, R. A. (1994) Structure of the RGD protein decorsin: conserved motif and distinct function in leech proteins that affect blood clotting. *Science* **264,** 1944-l947 CrossRef Medline

32. Koivunen, E., Wang, B., and Ruoslahti, E. (1994) Isolation of a highly specific ligand for the α5β1 integrin from a phage display library. *J. Cell Biol.* **124,** 373–80 CrossRef Medline

33. Cheng, S., Craig, W. S., Mullen, D., Tschopp, J. F., Dixon, D., and Pierschbacher, M. D. (1994) Design and synthesis of novel cyclic RGD-containing peptides as highly potent and selective integrin αIIbβ3 antagonists. *J. Med. Chem.* **37,** 1–8 CrossRef Medline

34. Aota, S., Nomizu, M., and Yamada, K. M. (1994) The short amino acid sequence Pro-His-Ser-Arg-Asn in human fibronectin enhances cell-adhesive function. *J. Biol. Chem.* **269,** 24756–24761 Medline

35. Mould, A. P., Askari, J. A., Aota, Si., Yamada, K. M., Irie, A., Takada, Y., Mardon, H. J., and Humphries, M. J. (1997) Defining the topology of integrin α5β1-fibronectin interactions using inhibitory anti-αv and anti-β1 monoclonal antibodies. Evidence that the synergy sequence of fibronectin is recognized by the amino-terminal repeats of the α5 subunit. *J. Biol. Chem.* **272,** 17283–17292 CrossRef Medline

36. Danen, E. H., Aota, S., van Kraats, A. A., Yamada, K. M., Ruiter, D. J., and van Muijen, G. N. (1995) Requirement for the synergy site for cell-adhesion to fibronectin depends on the activation state of integrin α5β1. *J. Biol. Chem.* **270,** 21612–21618 CrossRef Medline

37. Jovanović, J., Iqbal, S., Jensen, S., Mardon, H., and Handford, P. (2008) Fibrillin-integrin interactions in health and disease. *Biochem. Soc. Trans.* **36,** 257–262 CrossRef Medline

38. Weinreb, P. H., Simon, K. J., Rayhorn, P., Yang, W. J., Leone, D. R., Dolinski, B. M., Pearse, B. R., Yokota, Y., Kawakatsu, H., Atakilit, A., Sheppard, D., and Violette, S. M. (2004) Function-blocking integrin αvβ6 monoclonal antibodies: distinct ligand-mimetic and nonligand-mimetic classes. *J. Biol. Chem.* **279,** 17875–17887 CrossRef Medline